



Cite this: *J. Anal. At. Spectrom.*, 2019, **34**, 986

## Improved TIMS data reliability and precision with new ion source design

Herbert Siegmund,<sup>ID</sup>\*<sup>a</sup> Joe Hiess,<sup>ID</sup><sup>a</sup> Monika Sturm,<sup>a</sup> Andreas Koepf,<sup>a</sup> Christian L'Herault<sup>b</sup> and Sergej Boulyga<sup>a</sup>

The ion source design of the Triton and Triton Plus Thermal Ionisation Mass Spectrometer (TIMS) has been improved to reduce the frequency and intensity of high voltage electric sparking. Sparking can be caused by voltage flashover between the ion source components, resulting in rapid instability of the lens and acceleration voltages. This in turn leads to deflection of the ion beams in the analyzer and subsequently measurement biases, particularly on minor isotope detectors. Two prototype ion sources were engineered and tested to increase the condenser-to-ground flashover voltage without changing the geometry of any surfaces that would potentially adversely influence the ion beam transmission and focusing. The ion source enhancement facilitates better accuracy and precision of uranium total evaporation measurements. An external component test and analysis of natural uranium certified reference material 112-A has been used to validate the performance of three modified ion sources installed in two TIMS. The new design is commercially available.

Received 24th January 2019  
Accepted 8th March 2019

DOI: 10.1039/c9ja00032a

rsc.li/jaas

### 1. Introduction

Multi-collector sector-field mass spectrometers are well established and indispensable analytical tools in isotope ratio and isotope dilution analysis.<sup>1</sup> Due to the high precision and accuracy attainable with state-of-the-art multi-collector thermal ionisation mass spectrometry (MC-TIMS) instruments and comparatively few molecular and polyatomic interferences, MC-TIMS is considered a benchmark technique for isotope ratio analysis of numerous elements, and in particular for Sr, Nd, Ca, U, and Pu isotope and amount analysis.<sup>1–5</sup> The mass spectrometric analysis plays an important role in nuclear material accountancy as well as in the verification of declared inventories of U, Pu and Th element amounts and amounts of fissile uranium isotopes in facilities along all steps of the nuclear fuel cycle.<sup>4</sup> Therefore, MC-TIMS is widely applied at IAEA safeguards laboratories<sup>5,6</sup> as well as at research institutions and nuclear facilities worldwide for uranium and plutonium analysis,<sup>5–15</sup> including certification of reference materials.<sup>14–18</sup>

Over the past decades a number of significant improvements, both technical and procedural, have been made that have turned out to be very useful and advantageous for nuclear safeguards related analyses. Thus, the simultaneous multi-collection of isotopes allowed the implementation of the so-called “total evaporation” (TE) method,<sup>19–24</sup> for which the

sample is completely evaporated within a relatively short measurement time, thus minimizing the isotope mass fractionation effects and thereby reducing the measurement uncertainties. This technique is the most frequently used method today for analysis of U, and Pu isotope ratios as well for determination of concentrations of these elements in samples by isotope dilution mass spectrometry (IDMS).

In the TE method the purified uranium or plutonium nitrate solutions (with element amounts of 50 ng to 500 ng depending on the analysed element and on the applied procedure) are deposited onto a metal filament (made of tungsten or rhenium) and placed in the ion source of the mass spectrometer. Under computer control, ion currents are generated by heating of the filament(s). During the measurement process, the filament current is continuously adjusted in order to follow a predefined and reproducible evaporation profile. At the same time, all isotopes of interest are collected simultaneously during the entire period of evaporation. The ion currents are continually measured until the whole sample is exhausted. The final isotopic ratio is calculated from the measured ion currents of the respective isotopes that have been integrated over the course of the measurement.<sup>25,26</sup>

The isotope ratios produced from the integrated ion currents can be biased by spikes.<sup>†</sup> Thus, accordingly to Mathew *et al.*<sup>23</sup> occasionally electronic spikes are evident in the release profile of the isotopic abundances. The <sup>235</sup>U/<sup>238</sup>U ratio that includes the spike can be significantly biased, and therefore, the isotopic

<sup>a</sup>Department of Safeguards, IAEA – International Atomic Energy Agency, IAEA Laboratories Seibersdorf, Friedensstrasse 1, 2444 Seibersdorf, Austria. E-mail: H. Siegmund@iaea.org

<sup>b</sup>Thermo Fisher Scientific, 91963 Courtaboeuf, France

<sup>†</sup> In this article we define **electric sparking** or **flashover** as the physical effect of an ignition due to high voltage. While **signal spiking** is defined as unusual high or low transient artefacts in consecutive data points.

abundance profile and ratio profile from TE must be evaluated to examine if spikes attributable to electronic noise are present. According to the observations of the authors of this work in particular, minor isotopes of uranium ( $^{234}\text{U}$ ,  $^{236}\text{U}$ ) can also be strongly influenced by the presence of the spikes.

The aims of this study are to (1) investigate the reasons for the occurrence of electric sparking† in the ion source of MC-TIMS Triton and Triton Plus, (2) develop an approach to improve the ion source design so that the electric sparking could be reduced, and (3) validate the modified source by an external component test and analysis of appropriate quality control samples to ensure that significant effects were eliminated. The ultimate goal is to improve the precision, accuracy and efficiency of TIMS total evaporation technique through a significant reduction of the number of outliers in isotope ratio measurements and reduction in the frequency of failed analyses. Recent improvements to TIMS ion source design were also presented in ref. 27.

## 2. Experimental

### 2.1. Certified Reference Material (CRM)

Uranium isotopic standard NBL CRM 112-A (New Brunswick Laboratory, U.S. Department of Energy, USA), was used as a quality control (QC) sample.

### 2.2. Analytical equipment and measurement procedure

Multi-collector thermal ionization mass spectrometers (MC-TIMS) Triton and Triton Plus™ (Thermo Fisher Scientific, Bremen, Germany) were used for TE isotopic ratio measurements of uranium. Analytical procedures followed those described in ref. 5. All instruments are housed at the Nuclear Material Laboratory (NML) of the International Atomic Energy Agency (IAEA) in Seibersdorf, Austria. The MC-TIMS instruments used are equipped with nine Faraday cups and a discrete dynode secondary electron multiplier (SEM) detector. The detector configuration was adjusted for simultaneous recording of ions with mass-to-charge ratio of 233, 234, 235, 236, 237 and 238U (corresponding to ions  $^{233}\text{U}^+$ ,  $^{234}\text{U}^+$ ,  $^{235}\text{U}^+$ ,  $^{236}\text{U}^+$ ,  $^{237.05}\text{U}^+$  and  $^{238}\text{U}^+$ , respectively). Each Faraday cup detector was connected to a  $10^{11}$  or  $10^{12}$   $\Omega$  amplifier (the latter can be used for recording  $^{234}\text{U}^+$  and  $^{236}\text{U}^+$  ions). Amounts of sample solutions containing approximately 0.5  $\mu\text{g}$  of uranium in 1  $\mu\text{L}$  1 M nitric acid were loaded by pipette onto tungsten ribbon evaporation filaments (GERADTS GMBH, Bremen, Germany) and oxidized by applying a current of 1.0 A for 300 s and 2.4 A for 60 s. Each sample loaded evaporation filament was then partnered with a degassed rhenium ribbon ionization filament (GERADTS GMBH, Bremen, Germany) in a double filament assembly on the turret. The turret can hold a total of 42 filaments, paired over 21 measurement positions. The TE measurements were normally run as automated sequences. An amplifier gain calibration was made at the beginning of each sequence and an amplifier baseline measurement was performed at the start of each filament analysis. Once the ionization filament reached a target intensity of 70 mV, Re ion focusing on the  $^{187}\text{Re}$  signal was performed, followed by peak centering for the Re mass

calibration. The evaporation filament was then ramped up to 250 mV to focus on  $^{238}\text{U}$  signal and peak centered. At a voltage intensity of 0.5 V ( $^{238}\text{U}$  signal) data collection was started. The evaporation current was further ramped and regulated to provide a summed target intensity for the selected U isotopes of 10 V. The integration time of 1.049 seconds corresponds to one measurement cycle. The measurement stopped once the summed intensity dropped below 0.5 V.

### 2.3. Data inspection process

Each filament analysis was first assessed with the Thermo Triton Data Evaluation software package version 3.2.1.10 to examine the signal profiles for ion signal intensity and ratios. Measurements were then processed with the IAEA in-house developed Mass Spectrometry Data Evaluation Software (MSDES) version 4.0.12 and copied into in-house developed Quality Control tables and charts. No corrections were applied to the data to correct for instrumental mass fractionation, that is, all measurements were automatically corrected by the Triton software for baseline and gain calibration, and then reported as raw results, without further normalisation or tailing corrections.

### 2.4. Additional test equipment

A custom designed and constructed high-vacuum oven was used to bake each ion source at less than  $10^{-5}$  mbar and 170 °C for six hours. This was performed prior to installation in the Triton mass spectrometers where the ion source subsequently underwent an additional six hours of source baking following the standard Triton PCL script in the ion source vacuum chamber.

A PicoScope 4424 oscilloscope, with multiple trigger event memory and time stamp information was connected *via* a 1:1000 high-voltage probe to the Triton's 10 kV acceleration voltage (Fig. 1).

A Megger MIT 1020/2 (0–10 kV) high-voltage isolation tester was connected to each ion source as an external test to determine their condenser to ground electric flashover potential under atmosphere.

### 2.5. Precautions

Measurements carried out at the high-voltage systems are associated with hazard. Only appropriately trained and qualified personnel is allowed to work with high-voltage equipment.

## 3. Investigation of electric sparking occurrence in original ion sources

### 3.1. Occurrence of electric sparking

In a TIMS ion source a small fraction of the filament ribbon material and all of the loaded sample materials are evaporated and partially ionized in a close proximity to high-voltage lenses that serve for the extraction and focusing of the produced ions. Under certain conditions this cloud of the evaporated material

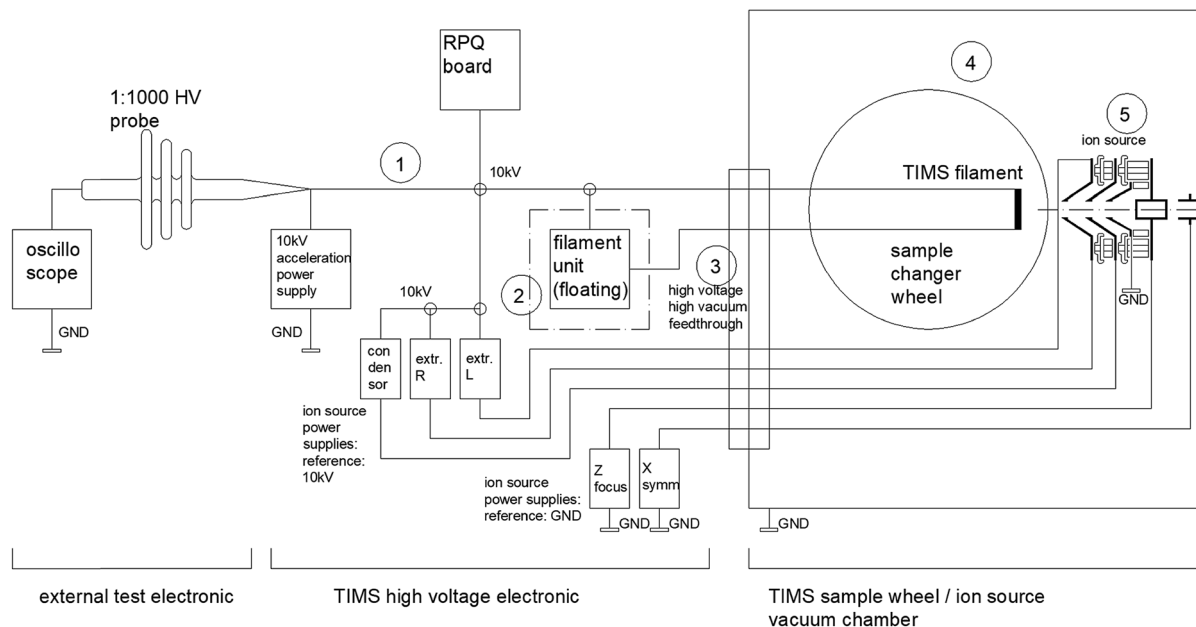


Fig. 1 Simplified schematic diagram demonstrating the monitoring of the high voltage in a TIMS Triton with an oscilloscope as applied in this study. Be aware of high-voltage hazards. Circled numbers 1 to 5 relate to potential sources of electric sparking as discussed later in Section 3.2 and Table 1.

could initiate electric sparking or flashover between the components of the ion source.

The produced electric sparks cause a very short-term instability of the lens voltages, and also influence the acceleration voltage of MC-TIMS Triton, usually by making it decrease, then increase and overshoot during a very short period of time. Such a sudden sag of acceleration voltage acts like an unwanted ultra-fast mass scan. The ion beams are deflected and sweep over other detectors in the multi-collector array (Fig. 2). Strong ion signals, such as  $^{238}\text{U}^+$ , hit detectors that are used for monitoring ions with lower masses (e.g. minor isotopes of uranium) in the cup configuration.

The electric sparks are very short and can be identified by a typical signal spiking pattern in the raw data as shown in Fig. 3, measurement cycle 548 and 1018. The typical signature of the events that produce a “sparking fingerprint” are described as:

- The intensity on the major  $^{238}\text{U}$  isotope decreases (Fig. 3a);
- The intensities of minor isotopes  $^{234}\text{U}$  and  $^{236}\text{U}$  increase significantly. Note that a signal spike is also observed at  $m/z = 237.05$  which is used in this study as a spark indicator (Fig. 3b);
- The intensity of  $^{235}\text{U}$  isotope may either decrease or increase (the latter shown in the Fig. 3b example) because on one hand during the transient spark event the  $^{235}\text{U}$  signal is

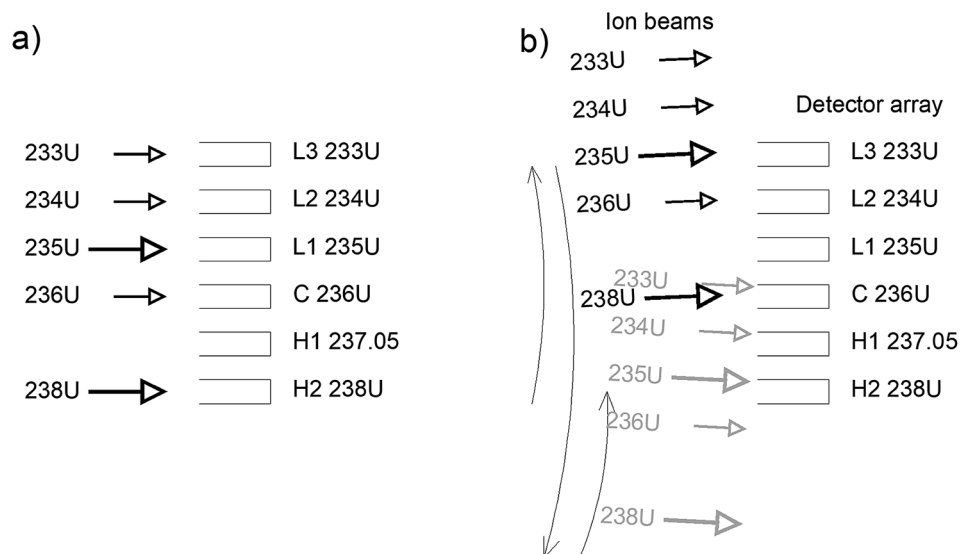


Fig. 2 Schematic diagrams showing (a) stable ion beams under normal conditions, and (b) sweeping ion beams during a sparking event.

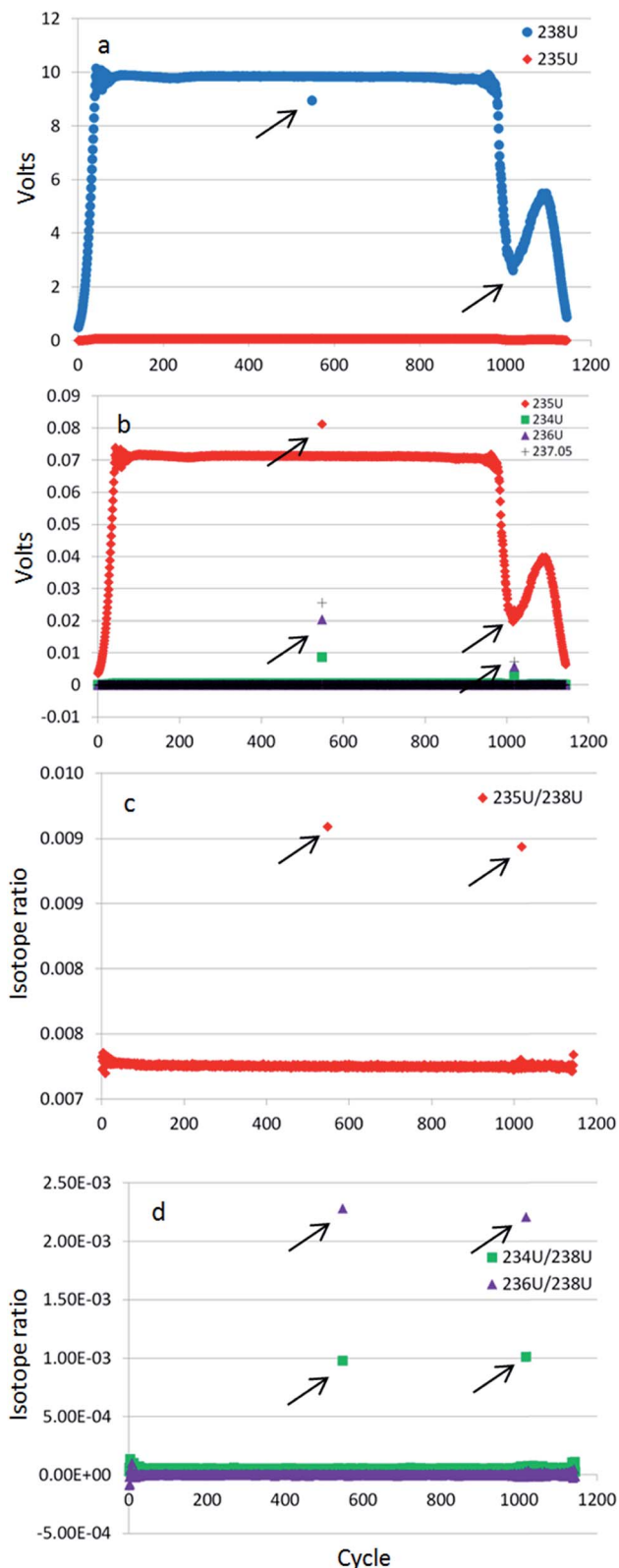


Fig. 3 Isotope signal strength and isotope ratio profiles generated during a single CRM 112-A TE measurement. Sparking events exhibit (a) an intensity drops of  $^{238}\text{U}$ , here at cycles 548 and 1018 as indicated with arrows; (b) simultaneous intensity gains of minor isotopes  $^{234}\text{U}$  and  $^{236}\text{U}$ , 237.05, and in this example also  $^{235}\text{U}$  occur. These result in sporadic increases in the (c)  $^{235}\text{U}/^{238}\text{U}$  ratio and (d)  $^{234}\text{U}/^{238}\text{U}$  and  $^{236}\text{U}/^{238}\text{U}$  ratios at the correlated cycles when sparking occurs. Each

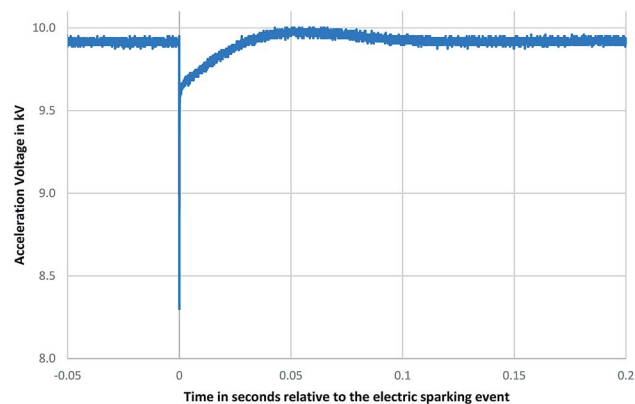


Fig. 4 A typical high-voltage spike in the acceleration voltage as recorded on the oscilloscope (see Fig. 1) due to flashovers. The horizontal axis covers a time interval of approximately 0.25 seconds. This time axis range therefore represents only a fraction (approximately a quarter) of a complete 1.049 second cycle exactly when a signal spike in the TE data plot also occurs, with an exactly matching time-stamp. Each cycle is represented as a single symbol in Fig. 3.

deflected away but on the other hand the respective detector records some variable amount of ions from the deflected  $^{238}\text{U}$  ion beam.

– The major  $^{235}\text{U}/^{238}\text{U}$  isotope ratio (Fig. 3c) as well as the minor  $^{234}\text{U}/^{238}\text{U}$  and  $^{236}\text{U}/^{238}\text{U}$  isotope ratios (Fig. 3d) are biased according to the corresponding sparking intensity.

A PicoScope 4424 oscilloscope with multiple trigger event memory was connected *via* a 1:1000 high-voltage probe to the Triton's 10 kV acceleration voltage to provide even more detailed sparking information (Fig. 1). The graph in Fig. 4 shows the sudden drop of the acceleration voltage, a typical pattern for electric sparks. The spark itself is very short ( $\ll 1$  ms). The acceleration voltage then rises, but overshoots and needs a few hundred milliseconds to stabilize again. There is an initial period of too low and then a later period of too high voltage after the spark. The change of acceleration voltage changes the kinetic energy of the ions and therefore their trajectory in the magnetic sector.<sup>28</sup> As this happens in an uncontrolled and unpredictable manner there is no programmed beam blanking performed, like in dynamic methods. The static TE method requires stable conditions.

When the acceleration voltage suddenly drops the ion beam is moved towards the lower mass region, but as soon as acceleration voltage is brought back by the control board it might slightly (by a few Volts) exceed the set value, which results in moving the ion beam into the opposite direction. Each sparking event recorded on the oscilloscope can be exactly correlated to the signal spiking in the TE data plots (Fig. 3) as a “sparking fingerprint” by their exactly matching timestamps. However, because the amplitude of the voltage drop differs from case to

cycle is represented as a single symbol and relates to an integration time of 1.049 seconds. This particular analysis corresponds to measurement number 15 in Fig. 8, 9 and 10, indicated there as the pink circled green diamond symbol made with the original ion source 472 on the Triton Plus T-4 instrument.

case the extent of the ion beam deviation from the target position can also be different.

### 3.2. Possible reasons of electric sparking related to the acceleration voltage

To trace and accurately identify the correct origin of sporadic sparking in complex high-voltage systems can be extremely difficult, especially when the frequency of such events is low, *i.e.* less than one event occurring per hour.

The oscilloscope (see Fig. 1) with multiple trigger event memory and time stamp recording was used to help record the sparking occurrence. Sparking was still detectable on the oscilloscope after disconnecting parts from the 10 kV line like the RPQ board or filament unit of the mass spectrometer or detuning the ion source voltages to a range where the ion signal was lost.

Table 1 describes the potential sources of electric discharges that were taken into account (see also Fig. 1).

We could see that as soon as the condenser lens voltage was reduced, the spiking on the acceleration voltage stopped. When the condenser lens voltage was increased, the spiking on the acceleration voltage was significantly more pronounced. This could be clearly observed by the amount of spikes detected on the oscilloscope, even if the ion signal was not detected any more due to de-tuning of ion lenses.

Sparking events inside the ion source could also be observed visually through the pyrometer portal window to the source chamber when the pyrometer and turret were removed and the condenser voltage was significantly increased.

The condenser to ground sparking was identified as the weakest point and could not be repaired by replacing the ion source. Seven clean and previously unused sources were baked in a high-vacuum oven and subsequently tested in the Triton Plus instrument. All showed the same behaviour as demonstrated for ion sources 472, 297, 343 and 431 in Table 2 and Fig. 8–10.

### 3.3. Detailed reasoning for sparking within the ion source from the condenser lens

The lenses of the ion source are made of thin stainless steel sheets. The condenser lens (Fig. 5) is positioned in close proximity to the filaments and has the highest potential difference (around 8000 V), towards the neighbour ground sheet. The heated filament ribbon evaporates material and locally reduces the vacuum level. At the weakest point on a nearby high-voltage lens the favourable conditions for a flashover can be reached. The dominant factors that influence this effect are: (1) the high-voltage potentials between separate lens sheets, (2) the narrow distances between them, (3) the sharpness of the material edges and (4) the local vacuum level. The isolation property of the condenser sheet to the neighbouring ground sheet was the weak point of the original ion-source.

## 4. Design improvements

Two prototype ion sources 507b and 481b were engineered and tested by the IAEA. Care was taken that the condenser-to-

**Table 1** Potential sources of electric discharge investigated in this study. Numbers 1 to 5 are also represented in Fig. 1

| Potential sources of electric discharges   | Effect description and expected symptoms  | Assessment                              |
|--|---|---|
| 1. Isolation damage outside vacuum chamber, cables, RPQ board <i>etc.</i>          | Isolation problems of cables <i>etc.</i> would show up as for example: burnmarks on the cables, problems disappearing when the cables are moved to other positions, or disappearing when parts of the system are disconnected ( <i>e.g.</i> the RPQ board).   | Not observed in this study              |
| 2. Filament-unit against ground  | The filament unit is floating on 10 kV, therefore the assembly is fully isolated. Isolation defects could lead to sporadic sparking   | Not observed in this study              |
| 3. Feedthroughs into vacuum chamber  | High-vacuum feedthroughs: metal or other particles or traces on the ceramic body could lead to sparking. We replaced all feedthroughs but the problem did not disappear   | Feedthroughs were ok in our study       |
| 4. Turret/cable assembly inside vacuum chamber                                     | The filament wheel is on 10 kV acceleration voltage potential, surrounded by the metal housing on ground potential. In case the supporting ceramic is not intact or shows burnmarks this would indicate a problem there. Wires inside the vacuum system sometimes have too close distances to each other or to ground                 | Not observed in this study              |
| 5. Ion source voltages (when power supplies are connected to acceleration voltage) | The ion extraction left and right and condenser lens voltages are not directly connected, but are referenced to the 10 kV acceleration voltage, see Fig. 1. Sparking of one of these ion source voltages to ground potential could also affect the acceleration voltage through the internal capacitor of the ion source power supply | Reason for signal spiking in this study |

**Table 2** Summary statistics from uranium isotopic ratio TE measurements made with different ion sources on TIMS Triton and Triton Plus. Bias values are calculated from "signal spikes" relative to "no signal spikes"

| Isotope ratio  | Mean                   | Bias    | SD                     | RSD    | Frequency    |
|--|------------------------|---------|------------------------|--------|--------------|
| <b>Original ion sources (472, 297, 343, 431) T4, signal spikes, n=63</b>     |                        |         |                        |        | <b>34.4%</b> |
| $^{234}\text{U}/^{238}\text{U}$  | $5.413 \times 10^{-5}$ | 1.817%  | $9.194 \times 10^{-7}$ | 1.699% |              |
| $^{235}\text{U}/^{238}\text{U}$  | $7.255 \times 10^{-3}$ | 0.020%  | $1.434 \times 10^{-5}$ | 0.020% |              |
| $^{236}\text{U}/^{238}\text{U}$  | $2.713 \times 10^{-6}$ | 291%    | $1.654 \times 10^{-5}$ | 61%    |              |
| <b>Original ion sources (472, 297, 343, 431) T4, no signal spikes, n=120</b> |                        |         |                        |        |              |
| $^{234}\text{U}/^{238}\text{U}$  | $5.316 \times 10^{-5}$ |         | $4.606 \times 10^{-7}$ | 0.866% |              |
| $^{235}\text{U}/^{238}\text{U}$  | $7.253 \times 10^{-3}$ |         | $7.322 \times 10^{-7}$ | 0.010% |              |
| $^{236}\text{U}/^{238}\text{U}$  | $6.943 \times 10^{-7}$ |         | $5.938 \times 10^{-7}$ | 86%    |              |
| <b>Prototype 507b T4, signal spikes, n=36</b>                                |                        |         |                        |        | <b>35.3%</b> |
| $^{234}\text{U}/^{238}\text{U}$  | $5.324 \times 10^{-5}$ | 0.185%  | $3.204 \times 10^{-7}$ | 0.602% |              |
| $^{235}\text{U}/^{238}\text{U}$  | $7.254 \times 10^{-3}$ | 0.001%  | $7.346 \times 10^{-7}$ | 0.010% |              |
| $^{236}\text{U}/^{238}\text{U}$  | $3.370 \times 10^{-7}$ | 163%    | $5.218 \times 10^{-7}$ | 155%   |              |
| <b>Prototype 507b T4, no signal spikes, n=66</b>                             |                        |         |                        |        |              |
| $^{234}\text{U}/^{238}\text{U}$  | $5.314 \times 10^{-5}$ |         | $3.835 \times 10^{-7}$ | 0.722% |              |
| $^{235}\text{U}/^{238}\text{U}$  | $7.253 \times 10^{-3}$ |         | $7.613 \times 10^{-7}$ | 0.010% |              |
| $^{236}\text{U}/^{238}\text{U}$  | $1.281 \times 10^{-7}$ |         | $4.614 \times 10^{-7}$ | 360%   |              |
| <b>524 T4, signal spikes, n=3</b>  |                        |         |                        |        | <b>2.9%</b>  |
| $^{234}\text{U}/^{238}\text{U}$  | $5.425 \times 10^{-5}$ | 1.992%  | $1.236 \times 10^{-6}$ | 2.278% |              |
| $^{235}\text{U}/^{238}\text{U}$  | $7.253 \times 10^{-3}$ | -0.005% | $3.904 \times 10^{-7}$ | 0.005% |              |
| $^{236}\text{U}/^{238}\text{U}$  | $9.996 \times 10^{-7}$ | 10%     | $6.278 \times 10^{-7}$ | 63%    |              |
| <b>524 T4, no signal spikes, n=101</b>                                       |                        |         |                        |        |              |
| $^{234}\text{U}/^{238}\text{U}$  | $5.320 \times 10^{-5}$ |         | $6.684 \times 10^{-7}$ | 1.257% |              |
| $^{235}\text{U}/^{238}\text{U}$  | $7.254 \times 10^{-3}$ |         | $8.942 \times 10^{-7}$ | 0.012% |              |
| $^{236}\text{U}/^{238}\text{U}$  | $9.125 \times 10^{-7}$ |         | $5.771 \times 10^{-7}$ | 63%    |              |
| <b>481b T2, signal spikes, n=4</b>   |                        |         |                        |        | <b>3.3%</b>  |
| $^{234}\text{U}/^{238}\text{U}$  | $5.373 \times 10^{-5}$ | 0.947%  | $6.284 \times 10^{-7}$ | 1.169% |              |
| $^{235}\text{U}/^{238}\text{U}$  | $7.253 \times 10^{-3}$ | -0.002% | $4.622 \times 10^{-7}$ | 0.006% |              |
| $^{236}\text{U}/^{238}\text{U}$  | $5.181 \times 10^{-6}$ | 397%    | $7.562 \times 10^{-6}$ | 146%   |              |
| <b>481b T2, no signal spikes, n=117</b>                                      |                        |         |                        |        |              |
| $^{234}\text{U}/^{238}\text{U}$  | $5.323 \times 10^{-5}$ |         | $6.695 \times 10^{-7}$ | 1.258% |              |
| $^{235}\text{U}/^{238}\text{U}$  | $7.254 \times 10^{-3}$ |         | $9.448 \times 10^{-7}$ | 0.013% |              |
| $^{236}\text{U}/^{238}\text{U}$  | $1.042 \times 10^{-6}$ |         | $7.914 \times 10^{-7}$ | 76%    |              |

ground flashover voltage was increased without changing the geometry of any surfaces that would influence the ion beam. No difference in behaviour of the source with respect to performance, tuning, *etc.* was expected. This development led to an enhanced ion source design that is now commercially available by the manufacturer Thermo Fisher Scientific, Bremen, Germany.

Three improvements were made in the enhanced ion sources:

(1) The shielding sockets or protecting umbrellas (see Fig. 5) are necessary to protect the ceramic isolators from evaporated material. Instead of the original conductive metal umbrellas, which were connected to condenser lens potential and showed a too narrow flashover distance to the ground sheet, the isolating umbrellas in the modified source were manufactured with ceramics or glass to prevent flashovers at this point.

(2) Sharp edges on the original metal parts could generate strong local electric field intensities and therefore high electron densities favouring flashover conditions. A mechanical rounding and polishing on these edges increased the radius and therefore reduced unwanted electric fields in the modified source.

(3) Removing material from the condenser support sheet increased the flashover distance to the ground sheet.

## 5. Validation of sparking performance indicator

Testing the functionality of a redesigned or modified ion-source for its sparking stability by using a mass spectrometer consumes valuable time and resources and reduces the availability of the TIMS instrument for any other analytical work. In order to avoid using the valuable analytical equipment, *i.e.* TIMS, during the prototyping process we developed a faster component test. The new test method was designed to quickly measure the flashover voltages from condenser to ground of different ion sources. The test can be done on a benchtop under atmospheric conditions (room temperature *ca.* 22 °C, *ca.* 60% humidity). Voltage is generated by a Megger MIT 1020/2 (0–10 kV) high-voltage isolation tester unit. The ion source is connected as shown in Fig. 6 and the voltage is increased slowly in fine steps, until the first spark ignites. Be aware of high-voltage hazards. This test should only be conducted by trained persons. The test is re-done at least 3 times, outliers removed, results averaged.

Fig. 7 presents the results of these tests conducted on several ion sources. Under atmospheric pressure the flashover voltages are lower than under vacuum, but such a test provides still a good comparison of different ion sources and serves as a quick indicator to assess sparking stability. The flashover voltage value can be used to index the arcing performance of a given ion source. Original ion sources recorded lower flashover voltages and typically correlated with a higher frequency and intensity of sparking leading to greater biases in their measured isotopic ratios as shown in Fig. 8–10, while modified ion sources recorded higher flashover voltages and improved performances in total evaporation test measurements.

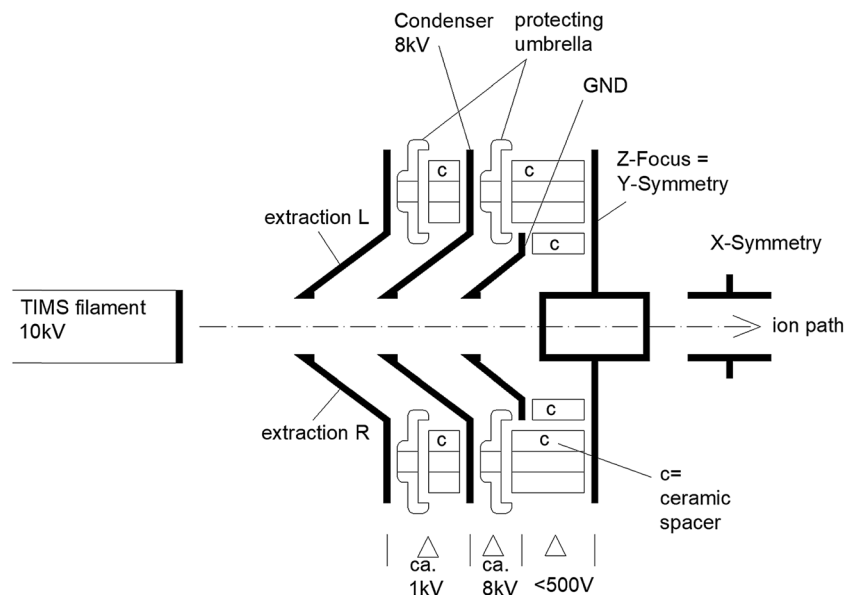


Fig. 5 Simplified schematic representation of a TIMS ion source (not to scale).

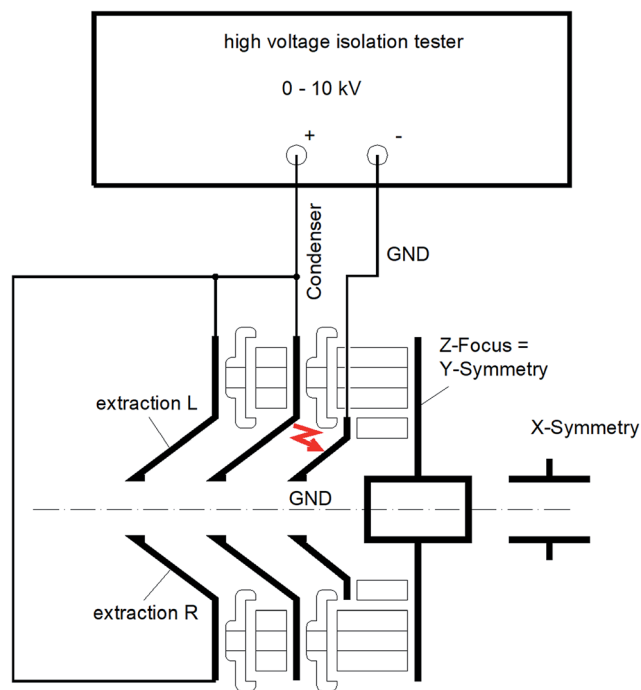


Fig. 6 Schematic diagram depicting connections for testing the ion source condenser to ground flashover voltage.

## 6. Other potential ion source high-voltage problems unrelated to the acceleration voltage

Failures in the high voltage of complex mass spectrometers can also occur for other reasons, but sometimes generate similar symptoms.

Although the effects described below were not observed in this study, we would like to mention such potential problems to avoid misinterpreting them.

For instance, when the ion source has been heavily used, material sprayed from the filament ribbon mainly builds up conductive layers on the front ceramics. Current can then start to flow through this layer to a neighbouring high-voltage sheet and drive the corresponding power supplies to their limits. This predominantly relates to the extraction left and right and condenser lenses as they are the most exposed. The applied voltages will no longer be stable and will detune the ion signal. This can lead to intensity drops like those shown in Fig. 3a, but it does not lead to an intensity gain on minor isotopes like in Fig. 3b. The acceleration voltage is not influenced and the ion beams do not sweep over the surrounding detectors as described in Fig. 2. Each isotope intensity drops more or less equally. The solution to this problem is simply to clean or replace these front ceramics.

## 7. Comparative performance of original and modified ion sources for U isotope ratio measurement by TIMS TE

### 7.1. Original ion source tests

Results of the original ion source tests (conducted on ion sources 472, 297, 343 and 431 with the TIMS Triton Plus (T-4)) can be found in the beginning of Table 2 and Fig. 8–10. In order to detect even minor signal spiking the ion intensity at  $m/z = 237.05$  (see Section 3.1 and Fig. 3b) was monitored and visually examined in the TE raw data. All measurement results, in which spikes at  $m/z = 237.05$  were observed are presented as green diamonds in Fig. 8–10. In total 183 filament measurements were made with these four ion sources. Signal spiking

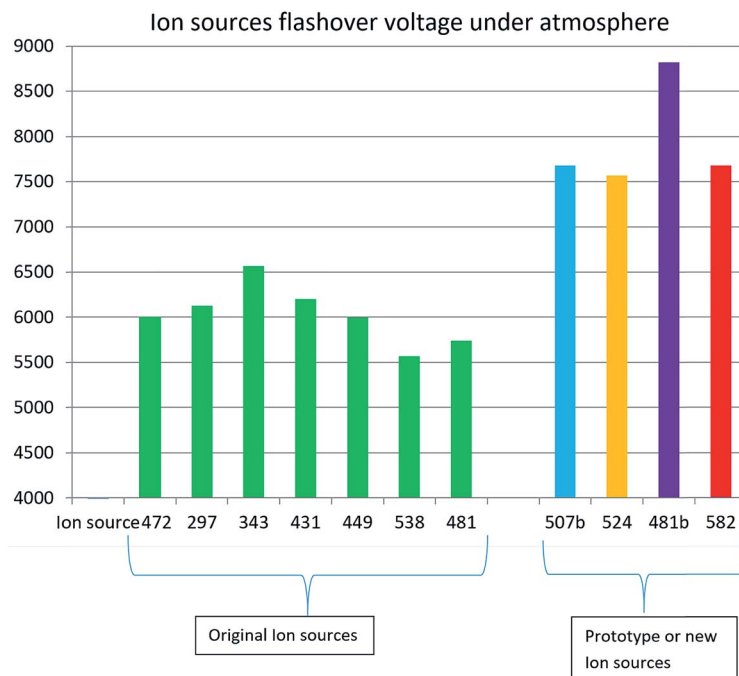


Fig. 7 Arcing performance as represented by flashover voltages from condenser to ground measured under atmosphere on a selection of ion sources. Seven green bars on the left are original ion sources. Modified ion sources are to the right. 507b and 481b are the IAEA prototypes, 524 and 582 are from the early modified serial production. Note the improvement for original ion source 481 following modification becoming 481b.

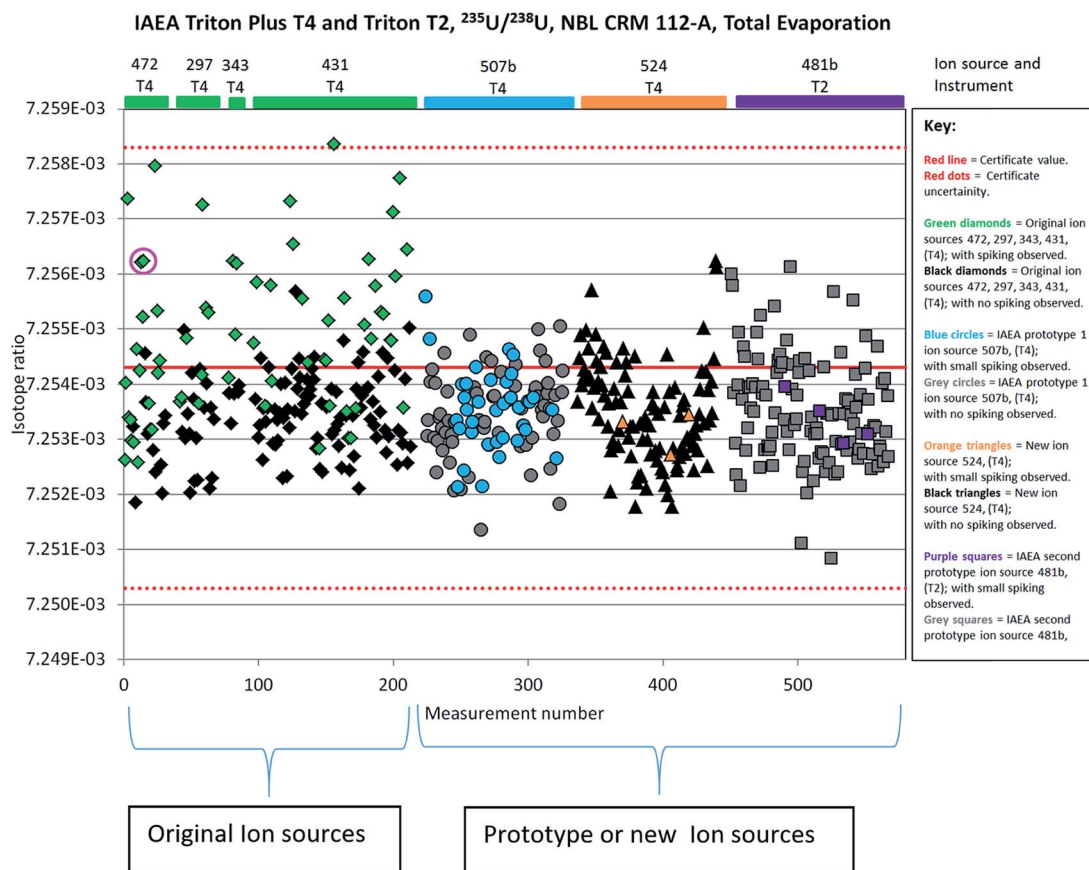


Fig. 8 QC chart displaying total evaporation  $^{235}\text{U}/^{238}\text{U}$  data collected on NBL 112-A certified reference material with various ion sources on the IAEA TIMS Triton Plus 'T4' and Triton 'T2'. Pink circled measurement discussed in Fig. 3.



was observed in 63 of these measurements leading to a high frequency (34.4%) of spiking events. The probability of the sparking was very irregular, but typically between 3 and 15 spikes occurred per turret. The effect of each sparking event on the measured isotope ratios is unique, *i.e.* we have never registered exactly the same change of isotope ratio during different sparking events. Sometimes multiple sparks can occur within a single measurement. Measurements that contain one or more sparking events are indicated with green diamonds in Fig. 8–10, while the measurements without sparking are indicated with black diamonds. Ratios of  $^{235}\text{U}/^{238}\text{U}$  (0.020%; Fig. 8) and  $^{234}\text{U}/^{238}\text{U}$  (1.817%; Fig. 9) are positively biased in the measurements with signal spiking with respect to measurements without signal spiking. Measurements with signal spiking also yielded higher relative standard deviations (RSD) than measurements without signal spiking for  $^{235}\text{U}/^{238}\text{U}$  (0.020% and 0.010% respectively) and  $^{234}\text{U}/^{238}\text{U}$  (1.699% and 0.866%) ratios. Note that CRM 112-A is not certified for a  $^{236}\text{U}/^{238}\text{U}$  ratio however the quoted value for the limit of detection of  $5 \times 10^{-9}$  from the certificate is marked as a red reference line in Fig. 10.

## 7.2. Modified ion source tests

Results of the modified ion source tests conducted on 507b and 524 with the Triton Plus TIMS (T-4) and 481b with the Triton TIMS (T-2) are presented in Table 2 and Fig. 8–10. In total 327 filament measurements were made with these three modified ion sources. As described above the ion intensity at  $m/z = 237.05$  (see Section 3.1 and Fig. 3b) was visually examined in the TE raw data to detect signal spiking. All measurement results, in which spikes at  $m/z = 237.05$  were observed are presented in Fig. 8–10 as blue circles, orange triangles and purple squares for ion sources 507b, 524 and 481b, respectively. Signal spiking was observed in 36 of the 102 measurements made on the very first prototype 507b leading to a high frequency (35.3%) of spiking events, similar to that observed with the original ion sources (see Section 7.1), but with much smaller intensities. However, despite the frequent small spikes observed at  $m/z = 237.05$  the measured U isotope ratios were not significantly biased, *i.e.* no measurable spikes were detected at  $m/z = 236.05$ ;  $m/z = 235.05$ ;  $m/z = 234.05$ . Obviously, the acceleration voltage drops were small and fast enough so that the very transient signal change was predominantly influencing the closest detector. Such an effect was

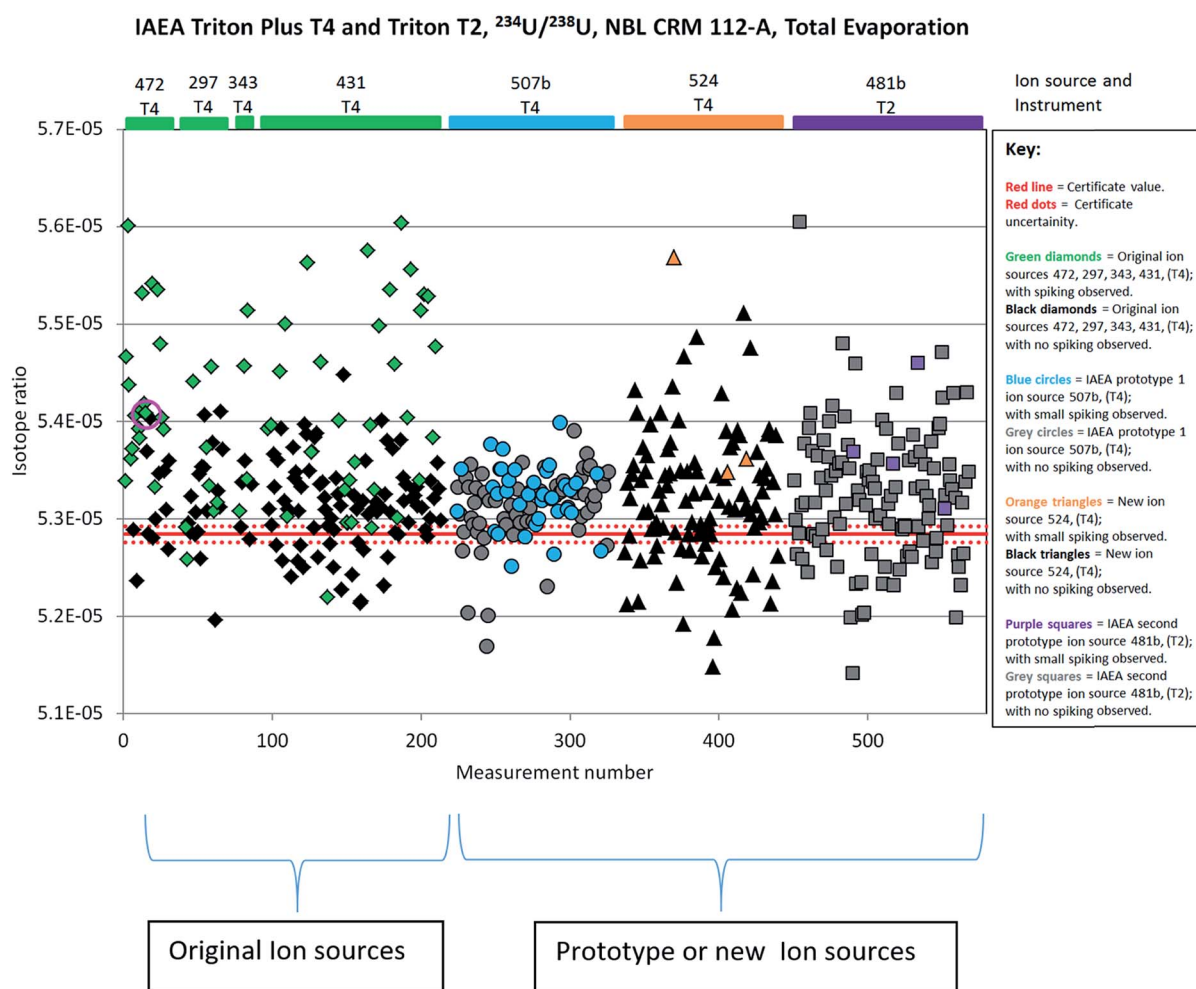


Fig. 9 QC chart displaying total evaporation  $^{234}\text{U}/^{238}\text{U}$  data collected on NBL 112-A certified reference material with various ion sources on the IAEA TIMS Triton Plus 'T4' and Triton 'T2'. Pink circled measurement discussed in Fig. 3.

only observed with the first prototype ion source 507b. The frequency of spiking events was significantly reduced in the case of ion sources 524 (3 of 104 measurements, or 2.9%) and 481b (4 of 121 measurements, or 3.3%). Measurements that contain one or more spiking events are indicated with blue circles (507b), orange triangles (524) or purple squares (481b) in Fig. 8–10, while measurements without noticeable spiking are indicated with grey or black symbols. In general, measurements of  $^{235}\text{U}/^{238}\text{U}$  ratios on the modified ion sources display negligible biases with respect to measurements without signal spiking (Fig. 8), which is in contrast to the larger bias seen on the original ion sources (see Section 7.1). However, measurements of  $^{234}\text{U}/^{238}\text{U}$  ratios with signal spiking appear still positively biased as compared to measurements without signal spiking (Fig. 9). Biases observed with ion sources 524 (1.992%) and 481b (0.947%) are similar to those obtained with the original ion sources, although their overall number is small ( $n = 3$  and 4). On the other hand, the bias observed in the case of ion source 507b (0.185%) is much less pronounced. When using the modified ion sources we did not find any systematic

effect of spikes on the measurement precision. In general, the precision (RSD) of the  $^{235}\text{U}/^{238}\text{U}$  ratio was better on the modified ion sources (0.005% to 0.013%) than for the original ion sources (0.02%).

All TIMS tests in this study were performed using TE measurements. However, sparks are even more likely to occur during “modified total evaporation” (MTE),<sup>14</sup> due to the higher signal level (higher temperatures) and greater amount of material loaded. Due to the longer integration times of MTE (usually 16 seconds) a sparking event might not be as clearly identified in the raw data. As the MTE method is more complex, a spark could cause a more complicated failure as it could happen any time during the MTE script and could also corrupt yield or tailing calculations. MTE is the method of choice for accurate minor isotope ratios. This study shows that sparking produces more bias on minor isotope ratios, therefore, elimination of such sparks is fundamental for reliable MTE data. Although the MTE data processing offers an outlier rejection, the frequent outliers generally expand the acceptance range by

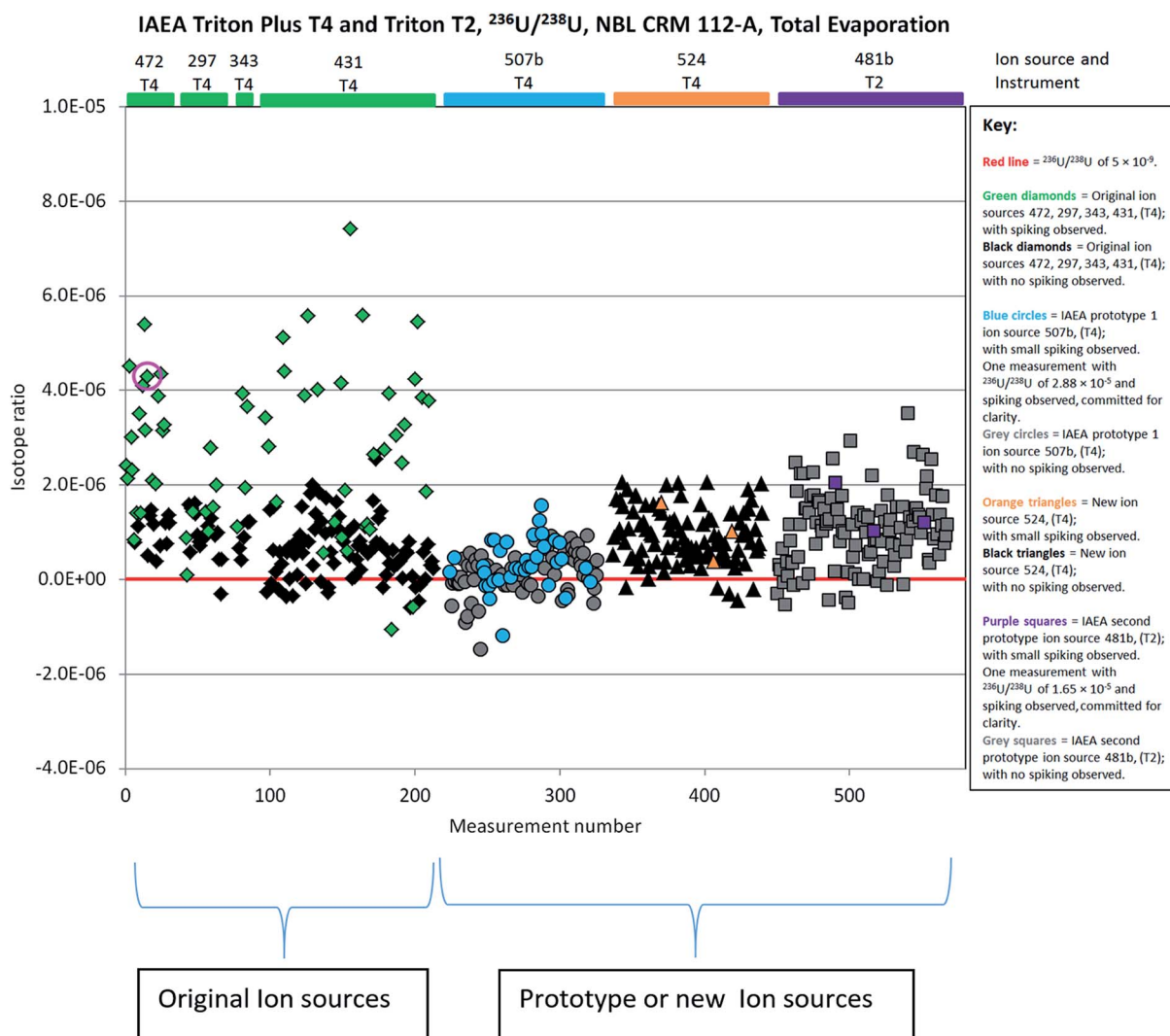


Fig. 10 QC chart displaying total evaporation  $^{236}\text{U}/^{238}\text{U}$  data collected on NBL 112-A certified reference material with various ion sources on the IAEA TIMS Triton Plus ‘T4’ and Triton ‘T2’. Pink circled measurement discussed in Fig. 3.

reducing measurement precision and they might still cause an undetected bias. Furthermore, often the outliers cannot be identified if a relatively long integration time (e.g. 8 to 16 s) is applied. Therefore, the physical elimination of signal spikes as done in this study significantly contributes to an improvement of robustness and accuracy of the measured isotope ratios.

## 8 Conclusion

Signal spikes that are caused by electrical sparking in the TIMS ion source cannot be identified and filtered out by the currently used TIMS data evaluation software. Therefore, they may result in more or less significant biases of the measured isotope ratios with a particular effect on minor U isotopes. The new ion-source design produced in cooperation between IAEA and Thermo Fisher Scientific prevents electric sparking. Application of this modified ion source results in a remarkable improvement of the repeatability and accuracy of U isotope ratio measured by using TIMS total evaporation technique. Also the frequency of outliers in TIMS TE measurements is significantly reduced, which improves the overall timeliness of analyses and reduces labour expenses of the analysts because fewer repetitions are required. The merits of the modified ion sources for TE measurements have been demonstrated by using MC-TIMS Triton and Triton Plus from Thermo Fisher Scientific.

## Conflicts of interest

The authors declare that one of the authors, Christian L'Herault, is employed by THERMO Fisher Scientific, the manufacturer of the TIMS instrument that is used in this study.

## Acknowledgements

The authors would like to acknowledge productive discussions with Hartmut Bars (THERMO Fisher Scientific) on the technical aspects of TIMS ion sources. The valuable comments of reviewers are appreciated.

## References

- 1 S. Burger, J. Vogl, U. Kloetzli, L. Nunes and M. Lavelle, Thermal Ionisation Mass Spectrometry, in *Sector Field Mass Spectrometry for Elemental and Isotopic Analysis, Book Series: New Developments in NMR*, ed. T. Prohaska, J. Irrgeher, A. Zitek and N. Jakubowski, Royal Soc Chemisitry, Cambridge, England, 2015, pp. 381–438.
- 2 J. M. Koornneef, C. Bouman, J. B. Schwieters and G. R. Davies, Use of 10(12) ohm current amplifiers in Sr and Nd isotope analyses by TIMS for application to sub-nanogram samples, *J. Anal. At. Spectrom.*, 2015, **28**, 749–754.
- 3 A. Heuser, A. D. Schmitt, N. Gussone and F. Wombacher, Analytical Methods, in *Calcium Stable Isotope Geochemistry, Book Series: Advances in Isotope Geochemistry*, ed. N. Gussone, A. D. Schmitt, A. Heuser, F. Wombacher, M. Dietzel, E. Tipper and M. Schiller, Springer-Verlag Berlin, Germany, 2016, pp. 23–73.
- 4 S. Boulyga, S. Konegger-Kappel, S. Richter and L. Sangély, *J. Anal. At. Spectrom.*, 2015, **30**, 1469–1489.
- 5 S. Bürger, S. D. Balsley, S. Baumann, J. Berger, S. F. Boulyga, J. A. Cunningham, S. Kappel, A. Koepf and J. Poths, Uranium and plutonium analysis of nuclear material samples by multi-collector thermal ionisation mass spectrometry: Quality control, measurement uncertainty, and metrological traceability, *Int. J. Mass Spectrom.*, 2012, **311**, 40–50.
- 6 K. Raptis, G. Duhamel, R. Ludwig, S. Balsley, S. Burger, V. Mayorov, A. Koepf, S. Hara, Y. Itoh, K. Yamaguchi, T. Yamaguchi and J. Ninagawa, Measurement of non-separated U/Pu samples: optimization of TIMS procedures for safeguards purposes at Rokkasho on-site laboratory, *J. Radioanal. Nucl. Chem.*, 2013, **296**(2), 585–592.
- 7 S. Bürger, L. R. Riciputi, D. A. Bostick, S. Turgeon, E. H. McBay and M. Lavelle, *Int. J. Mass Spectrom.*, 2009, **286**, 70–82.
- 8 R. Jakopič, S. Richter, H. Kühn and Y. Aregbe, *J. Anal. At. Spectrom.*, 2010, **25**, 815–821.
- 9 K. Mayer, M. Wallenius and I. Ray, *Analyst*, 2005, **130**, 433–441.
- 10 S. Usuda, K. Yasuda, Y. Saito-Kokubu, F. Esaka, C.-G. Lee, M. Magara, S. Sakurai, K. Watanabe, F. Hirayama, H. Fukuyama, K. T. Esaka, K. Iguchi, Y. Miyamoto and J.-Y. Chai, *Int. J. Environ. Anal. Chem.*, 2006, **86**, 663–675.
- 11 C. G. Lee, K. Iguchi, J. Inagawa, D. Suzuki, F. Esaka, M. Magara, S. Sakurai, K. Watanabe and S. Usuda, *J. Radioanal. Nucl. Chem.*, 2007, **272**, 299–302.
- 12 H. T. Zhang, F. R. Zhu, J. Xu, Y. H. Dai, D. M. Li, X. W. Yi, L. X. Zhang and Y. G. Zhao, *Radiochim. Acta*, 2008, **96**, 327–331.
- 13 M. Kraiem, S. Richter, H. Kühn and Y. Aregbe, *Anal. Chim. Acta*, 2011, **688**, 1–7.
- 14 S. Richter, H. Kühn, Y. Aregbe, M. Hedberg, J. Horta-Domenech, K. Mayer, E. Zuleger, S. Bürger, S. Boulyga, A. Köpf, J. Poths and K. Mathew, *J. Anal. At. Spectrom.*, 2011, **26**, 550–564.
- 15 S. Bürger, R. M. Essex, K. J. Mathew, S. Richter and R. B. Thomas, *Int. J. Mass Spectrom.*, 2010, **294**, 65–76.
- 16 K. J. Mathew, G. L. Singleton, R. M. Essex, A. Hasozbek, G. Orłowicz and M. Soriano, Characterization of Uranium Isotopic Abundances in Depleted Uranium Metal Assay Standard 115, *J. Radioanal. Nucl. Chem.*, 2013, **296**, 435–440.
- 17 K. J. Mathew, P. Mason, A. Voeks and U. Narayanan, Uranium Isotope Abundance Ratios in Natural Uranium Metal Certified Reference Material 112-A, *Int. J. Mass Spectrom.*, 2012, **315**, 8–14.
- 18 K. J. Mathew, R. M. Essex, A. Hasozbek, G. Orłowicz and M. Soriano, Uranium Isotope-amount Ratios in Certified Reference Material 116-A– Uranium (Enriched) Metal Assay and Isotopic Standard, *Int. J. Mass Spectrom.*, 2014, **369**, 48–58.
- 19 S. F. Romkowski and L. Koch, *Proceedings to Eight Annual ESARDA Symposium, 12–14 May, 1987*, London.
- 20 R. Fiedler, D. Donohue, G. Grabmueller and A. Kurozawa, *Int. J. Mass Spectrom. Ion Processes*, 1994, **132**, 204.

- 21 R. Fiedler, *Int. J. Mass Spectrom.*, 1995, **146/147**, 91–97.
- 22 E. L. Callis and R. M. Abernathy, *Int. J. Mass Spectrom.*, 1991, **103**, 93–105.
- 23 K. J. Mathew, G. O'Connor, A. Hasozbek and M. Kraiem, Total Evaporation Method for Uranium Isotope-amount Ratio Measurements, *J. Anal. At. Spectrom.*, 2013, **28**, 866–876.
- 24 M. R. Wegener, K. J. Mathew and A. Hasozbek, The direct total evaporation (DTE) method for TIMS analysis, *J. Radioanal. Nucl. Chem.*, 2013, **296**(1), 441–445.
- 25 D. Tuttas, *Total Sample Evaporation of 1 ng SRM U350. Application Note 30017*, Thermo Fisher Scientific, Bremen, Germany, <https://assets.thermofisher.com/TFS-Assets/CMD/Application-Notes/AN-30017-ICP-MS-SRM-U350-Evaporation-AN30017-EN.pdf> downloaded on 2017-11-10.
- 26 ASTM C1672 – 17, Standard Test Method for Determination of Uranium or Plutonium Isotopic Composition or Concentration by the Total Evaporation Method Using a Thermal Ionization Mass Spectrometer.
- 27 A. Basak, R. K. Bhatia, V. K. Yadav, E. Ravisankar, T. K. Saha, V. Nataraju and S. C. Gadkari, *Int. J. Mass Spectrom.*, 2017, **423**, 33–38.
- 28 L. Rottmann, N. Jakubowski, S. Konegger-Kappel, O. Hanousek and T. Prohaska, Technical Background, in *Sector Field Mass Spectrometry for Elemental and Isotopic Analysis, Book Series: New Developments in NMR*, ed. T. Prohaska, J. Irrgeher, A. Zitek and N. Jakubowski, Royal Soc Chemistry, Cambridge, England, 2015, pp. 44–96.